International Journal of Research Publication and Reviews

Evaluating the Antitubercular Potential of Tinospora Crispa (Makabuhay): In Silico Approaches to Identify Bioactive Compounds Against Mycobacterium Tuberculosis

Reese Andrea L. Caguco[1], Mary Angelyn P. Deligero[2], Catherine Jasmine M. Dima-ano[3], Sherwin S. Fortugaliza, Ph.D.[4]

[1,2,3]UG Student, [4]Research Adviser
Davao City National High School
DOI : https://doi.org/10.55248/gengpi.6.0225.0962

ABSTRACT

Mycobacterium tuberculosis (Mtb) remains a significant global health challenge, necessitating the discovery of novel therapeutic agents to combat its rising resistance to conventional antibiotics. This study investigates the molecular docking analysis of phytochemicals derived from Tinospora crispa (Makabuhay) against key proteins associated with Mtb, employing AutoDock Vina for in silico evaluation. A comprehensive library of 40 phytochemical compounds from Tinospora crispa was screened, revealing several promising candidates. The analysis identifies the top-ranking compound, which displayed a binding affinity of -8.7 kcal/mol, indicating strong potential for interaction with the Mtb proteins. In particular, specific phytochemicals demonstrated significant binding to crucial active sites involved in Mtb pathogenesis, thereby suggesting their potential as inhibitors of bacterial entry and survival. The interactions of these phytochemicals with critical residues were elucidated, highlighting the role of hydrogen bonds and hydrophobic interactions in enhancing binding stability. These findings emphasize the therapeutic promise of Tinospora crispa-derived phytochemicals in targeting Mtb and pave the way for future experimental validation. Furthermore, the study underscores the importance of exploring natural compounds for innovative drug development strategies against tuberculosis, particularly in an era of increasing antimicrobial resistance. Molecular docking serves as a vital tool in the early stages of drug discovery, providing insights into protein-ligand interactions that can guide the development of effective antitubercular agents.

KEYWORDS: Mycobacterium tuberculosis, Molecular Docking, Tinospora crispa, Phytochemicals, AutoDock Vina

Introduction

Mycobacterium tuberculosis causes tuberculosis, which continues to remain a global health crisis. The World Health Organization, for example, reports approximately 1.5 million deaths and 10 million new infections annually (WHO, 2023). The emergence of multidrug-resistant and extensively drug-resistant TB strains presents a significant danger to the global drive toward TB control (Pitaloka et al., 2021). Being heavily reliant on a few, which are ineffective nowadays due to the development of resistance mechanisms, contemporary treatments badly need new therapeutic agents capable of overcoming such mechanisms.

Tuberculosis has been a human pathogen for almost 9,000 years, according to the CDC (2023), based on discovering human remains from ancient cultures. Traditionally known as "consumption" because of severe weight loss, TB was the leading killer in Europe and North America in the 18th and 19th centuries. According to the CDC, the discovery by Robert Koch of Mycobacterium tuberculosis in 1882 overthrew prevailing views that caused hereditary infections, transforming the understanding of TB towards airborne transmission and laying the pathway to modern public health efforts.TB primarily spreads through droplets from individuals with active pulmonary infections (WHO, 2023). Once inhaled, the bacteria reach the lungs and evade the immune system by surviving inside alveolar macrophages (Iseman et al., 2017). While many people harbor latent TB, the risk of reactivation is 5-10%, especially for those with compromised immune systems, such as individuals with HIV (CDC, 2023).

The treatment regimens for TB are complex and challenging to administer. The most commonly used anti-TB antibiotics developed in the mid-20th century are a principal mainstay of therapy. Anti-TB regimens vary with the stage and anatomic location of the infection, the immune status and age of the host, the presence of comorbidities, the development of toxicities, drug-drug interactions, and resistance patterns of the bacterium (Flint et al., 2020). Resistance to antibiotics is growing; treatment usually requires new antibiotic combinations that have been tried in fewer clinical trials than needed for adequate proof of efficacy. Therapy must run much longer than has traditionally been the case to eradicate *M. tuberculosis* (Stadler et al., 2023) Prevention of TB poses an enormous challenge since the disease is relatively easy to transmit.

In contrast, conditions that help in its transmission include poverty, overcrowding, and low-capacity public health infrastructure. Nonspecific symptoms such as chronic cough are often not reported, leading to high rates of transmission. Even in settings with well-functioning public health infrastructures, multiple antibiotics for a long time could be a challenge. Areas with a high prevalence of TB often lack adequate public health resources, as the COVID-19 pandemic illustrated.

TB remains one of the principal public health problems in the Philippines, with the highest incidence rate worldwide of 554 cases per 100,000 population (Department of Health, 2023). With the prevalence of MDR-TB among new patients being estimated at 4.1% and in previously treated cases at 21%, this further confronts the conventional treatment regimen for TB infection (WHO, 2023). There is an apparent scarcity of literature that talks about potential indigenous Philippine medicinal plants as alternative treatments amidst the country's rich biodiversity. Strains of drugs continue to rise, and there is a need to study new therapeutic alternatives that may be derived from natural sources. The local TB situation in Davao City mirrors the national trend, with alarmingly increasing cases of drug-resistant TB.

Alcaraz et al. (2022) reported that of the newly diagnosed cases in the region, 3.7% are resistant, while 20% of previously treated cases are resistant to first-line TB drugs. Even though the country is rich in medicinal plants like *Tinospora crispa* (Makabuhay), more scientific studies on their antitubercular properties need to be done. *Tinospora crispa* has antimicrobial, anti-inflammatory, and antioxidant activities. It is under-explored as a source of new compounds against TB. It has opened a significant research gap in investigating the indigenous plants that can cure MDR-TB. Studies have shown that in silico approaches are practical tools in TB drug discovery.

Pitaloka et al. applied molecular docking and dynamics simulations to screen quercetin analogs as inhibitors of the critical enzyme, enoyl-acyl carrier protein reductase (InhA), in *M. tuberculosis* fatty acid biosynthesis. Their results demonstrated the capability of computational methods in identifying potential candidates for drugs by letting them interact with the bacterium's enzymes. Similarly, Yan et al. (2022) highlighted the importance of immune evasion mechanisms and resistance in *M. tuberculosis*, such that overall mechanisms should be targeted to take recourse to newer strategies such as silico drug design to discover novel antitubercular compounds. These computational methods help identify promising drug candidates and enable screening large chemical libraries that would otherwise be time-consuming and costly compared to traditional drug discovery paradigms (Caws et al., 2020).

In silico approaches are gaining recognition as pivotal for the development of new approaches to deal with TB in light of continued medical resistance against drugs and the immediate need for new therapeutics.

Tinospora crispa (L.) Hook. f. Thomson, commonly referred to as Makabuhay, is an indispensable medicinal plant in the Philippines, as it is being used for vast therapeutic purposes in traditional medicines. It is a climbing plant of the family Menispermaceae found in tropical regions and has been used for generations by different ethnic groups in fighting and curing various diseases.

Makabuhay has curative applications against health conditions like fever, digestive disorders, and other diseases related to the respiratory tract. Preparations in the form of an aqueous extract or decoction reduce health conditions such as flatulence, indigestion, diarrhea, and inflammatory disorders due to rheumatism and arthritis (Quisumbing, 1978; Dhedhi et al., 2021). Of particular interest is that the herb is used as a folk remedy against tuberculosis and various other infectious diseases, which further signifies the importance of the plant in local health care. *T. crispa* contains many bioactive compounds such as alkaloids, flavonoids, terpenoids, and glycosides that give its pharmacological activities.

Alkaloids exhibit analgesic and anti-inflammatory effects, whereas flavonoids are known antioxidants with the potential to bring pain relief to inflammation. Antimicrobial activities have been associated with the action of terpenes (Benyamin et al., 2008; Hipol et al., 2022). Recent scientific research has tried to justify such applications by testing the plant for anti-inflammatory and analgesic activity, establishing its prospect as an adjunct therapy for chronic diseases (Dhedhi et al., 2021). With this in mind, this paper is going to review whether it can serve as a potential drug against drug-resistant pathogens, like *Mycobacterium tuberculosis*, and thus, reinforce its role in modern clinical practice.

Ligands derived from Makabuhay shall be docked against the TB biosynthesis-related protein 1BVR-InhA. The binding affinities of the compounds above shall be compared with that of the classically prescribed first-line isoniazid drug to determine which ligands/biochemical compounds have the highest affinity for binding. This study addresses a gap in past research by conducting a holistic in silico appraisal of the antitubercular capability of *Tinospora crispa*. This research will identify and evaluate bioactive compounds from *Tinospora crispa* that might inhibit critical enzymes from *Mycobacterium tuberculosis* using virtual screening molecular docking and molecular dynamics simulations.

Advanced computation would be utilized in this work to produce a cost-effective and time-efficient method of drug discovery. This study would eventually lead to new therapeutic compounds that could help the global fight against TB in drug-resistant forms. The local medicinal plants and their applications to TB will further scientific knowledge, providing a new perspective on drug discovery from plants importance in local healthcare practices.

This study aims to investigate the selected phytochemicals from Makabuhay in inhibiting TB through molecular docking analysis utilizing AutoDock Vina. Specifically, the researchers' objectives are to:

I. Identify and isolate phytochemical compounds from Tinospora crispa with potential antitubercular activity.

II. Evaluate the binding affinity of these compounds against key targets in Mycobacterium tuberculosis through molecular docking studies.

III. Assess the potential immunomodulatory effects of these compounds on immune response markers associated with TB.

IV.   Provide insights into the potential of Tinospora crispa as a source of new antitubercular agents for further pharmacological investigation.

2. Methodology

Screening and Preparation of Phytocompounds from Tinospora crispa

Forty-one primary phytochemicals from Tinospora crispa (Makabuhay) were selected for evaluation based on their reported pharmacological potential, particularly in treating infectious diseases such as tuberculosis (TB). These compounds were initially screened for drug-likeness using Lipinski's rule of five, a widely accepted method for determining the likelihood of a compound being orally active in humans. This rule, which is applied through SwissADME (http://www.swissadme.ch), ensures that each compound adheres to the following criteria: no more than 5 hydrogen bond donors (calculated by the number of nitrogen-hydrogen and oxygen-hydrogen bonds), no more than 10 hydrogen bond acceptors (all nitrogen and oxygen atoms), a molecular weight less than 500 Daltons, and an octanol-water partition coefficient (ClogP) not greater than 5 (Karami et al., 2022; Olatunde et al., 2022).

Compounds violating more than one of these parameters were excluded from further analysis. Lipinski's rule is critical as it predicts whether a compound has the necessary properties to ensure good bioavailability, solubility, and chemical stability, making it a useful predictor of a compound's potential to be developed into an orally administered drug.

Out of the 41 compounds, 34 passed the Lipinski's rule test. These filtered compounds were then prepared for molecular docking studies, a process that began by converting the compound structures from their initial SDF (Structure Data File) format into PDB (Protein Data Bank) format using PyMOL (Schrödinger, 2015). The conversion to PDB format is crucial as it allows for compatibility with docking software such as Autodock Vina. Each compound was then loaded into MGL AutodockTools (v.1.5.7), where essential pre-docking modifications were made. These modifications included the addition of Gasteiger charges, which are used in molecular docking to calculate the electrostatic interactions between the ligand and the protein. Additionally, the torsional degrees of freedom for each ligand were automatically set, allowing the ligand to rotate around its bonds during the docking simulation. Once optimized, each ligand was saved in PDBQT (PDB with charges and torsions) format, ready for docking.

Preparation of Protein (InhA) and Receptor Grid Box Manual Generation

The target protein in this study is the enoyl-acyl carrier protein reductase (InhA) from *Mycobacterium tuberculosis* (PDB ID: 1BVR), a key enzyme in the fatty acid biosynthesis pathway of the bacterium. Inhibiting InhA disrupts the production of mycolic acids, essential components of the bacterial cell wall, making it a promising target for antitubercular drugs. The 3D structure of InhA was downloaded from the Protein Data Bank (RCSB PDB, https://www.rcsb.org/) in PDB format. Once downloaded, the protein underwent energy minimization using the Swiss PDB Viewer (Tuli et al., 2022), which helps to relax the protein structure, removing any steric clashes or irregularities that could affect the accuracy of the docking process.

Following energy minimization, the protein was imported into MGL AutodockTools for further preparation. At this stage, all water molecules (which could interfere with the docking process) and other heteroatoms (non-standard molecules, such as ions or small solvent molecules) were removed. Polar hydrogens were added to the protein structure, and Kollman charges were applied. These charges are necessary to simulate the electrostatic interactions between the protein and the ligands during docking. The modified protein structure was then saved in PDBQT format, making it compatible with Autodock Vina for docking simulations.

Receptor Grid Box Manual Generation

To ensure that the docking simulations accurately targeted the active site of the InhA protein, a receptor grid box was generated around the binding site of the protein. This binding site was determined through literature and bioinformatics tools such as CASTp (Ali et al., 2018), which identifies pockets and cavities on the protein surface that could serve as potential binding sites. In the case of InhA, the active site is well-characterized, consisting of several crucial residues responsible for ligand binding and catalytic activity. These residues include SER 20, ILE 21, LEU 63, ASP 64, VAL 65, GLN 66, SER 94, ILE 95, GLY 96, PHE 97, LYS 165, ALA 191, GLY 192, PRO 193, ILE 194, and THR 196. Additionally, key hydrophobic and hydrogen bonding residues, such as PHE 41, ILE 122, PHE 149, MET 147, TYR 158, and MET 199, contribute to the binding specificity and affinity of ligands.

The grid box was manually set to dimensions of 70x70x70 Å³ to encompass the active site and surrounding residues, ensuring that the ligands had sufficient space to bind within the active pocket. The grid was centered at coordinates X: 19.050, Y: 18.992, and Z: 9.686, based on the position of the active site. By defining this grid box, the docking simulation could focus on the critical region of the protein, improving the likelihood of identifying high-affinity ligands. The grid size was deliberately chosen to minimize the risk of non-specific or irrelevant binding events outside the active site, which could lead to misleading docking results (Ali et al., 2018).
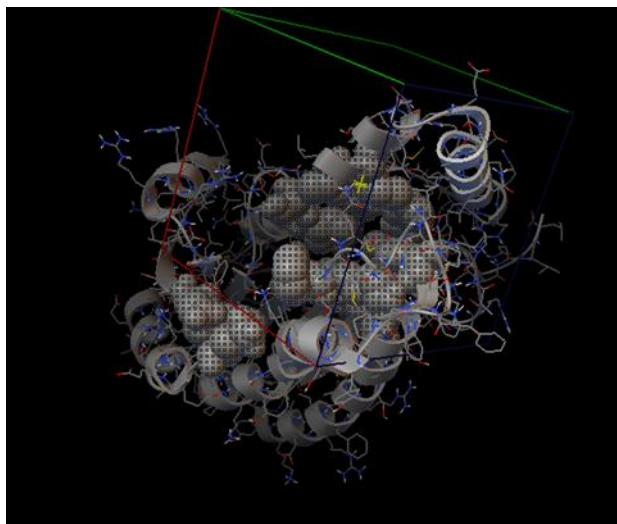
Fig 1. *Inha (PDB ID: 1bvr) receptor grid box visualization through MGL AutodockTools v. 1.5.7. Amino acids of the main binding site were set to appear as spheres.*

Molecular Docking Analysis and Simulation

The docking analysis and simulation were carried out after saving the optimized ligands, protein, and configuration files in the same folder. This process was executed using the Command Prompt on Windows 10 and 11 systems. Autodock Vina software was used for the docking via the Command Prompt. The directory was set to the folder containing the ligand, protein, and configuration files. The following command was entered to run the docking computation:

"C:\Program Files (x86)\The Scripps Research Institute\Vina\vina.exe" --receptor protein.pdbqt --ligand [ligand.pdbqt] --config [config.txt] --log [log.txt] --out [output.pdbqt]"

The docking process was performed ten times for each ligand, calculating the binding affinities of molecules docked to the Inha (PDB ID: 1BVR). The resulting output included log files in text format and output files in PDBQT format. After computation, the output and protein files were imported into PyMol for 3D simulation. Visualization tools such as UCSF Chimera, PyMOL, and Ligplot+ were used to display the docking interactions between proteins and ligands.

Scoring and Analysis

The scoring and analysis of the docking results focused on the binding affinity between the ligands and the active site residues of InhA (PDB ID: 1BVR). Binding affinity values were expressed in kcal/mol, with more negative values indicating stronger ligand-protein interactions. Out of the five docking runs conducted for each ligand, the pose with the lowest energy was selected for further analysis, as this conformation is expected to represent the most stable and favorable interaction between the ligand and the protein (Ali et al., 2018). The threshold binding affinity for considering a ligand as a potential inhibitor was set at -7 kcal/mol, with the reference drug isoniazid, having a binding affinity of approximately -6.4 kcal/mol, used as a benchmark.
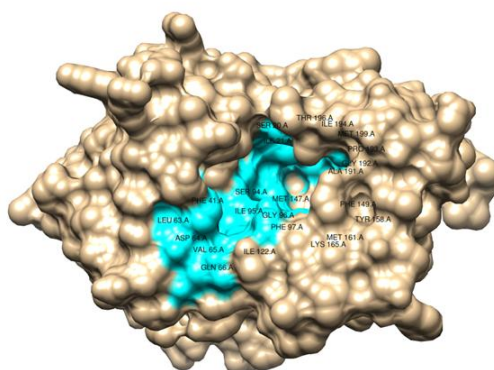

Fig 2. *Interacting residues of Inha (PDB ID: 1BVR)*

Key interacting residues within the active site of InhA were closely examined, particularly those involved in hydrogen bonding and hydrophobic interactions. These residues included SER 20, ILE 21, LEU 63, ASP 64, VAL 65, GLN 66, SER 94, ILE 95, GLY 96, PHE 97, LYS 165, ALA 191, GLY 192, PRO 193, ILE 194, and THR 196, along with other critical hydrophobic residues such as PHE 41, ILE 122, PHE 149, MET 147, TYR 158,

and MET 199. Hydrogen bonding residues like SER 20, GLY 96, and LYS 165 were especially important for stabilizing the ligands within the binding pocket, while hydrophobic interactions with residues such as PHE 97, MET 199, and ILE 194 further contributed to the overall binding strength.

The docking poses and interactions were visualized using PyMOL, providing a 3D representation of how each ligand fit into the active site of InhA. LigPlot+ was employed to generate 2D interaction maps, highlighting the specific hydrogen bonds and hydrophobic interactions that contributed to the binding affinity. Ligands showing strong interactions with critical residues like PRO 193, MET 199, and TYR 158 were prioritized for further investigation, as these residues are crucial for ligand stabilization. Additionally, ligands that formed hydrogen bonds with key residues such as GLY 96 and LYS 165 were considered promising due to the importance of these interactions in maintaining specificity within the binding pocket. Ultimately, ligands that demonstrated stronger binding affinity than isoniazid were considered potential lead compounds for inhibiting the InhA enzyme, thus presenting a viable pathway for the development of new antitubercular treatments.
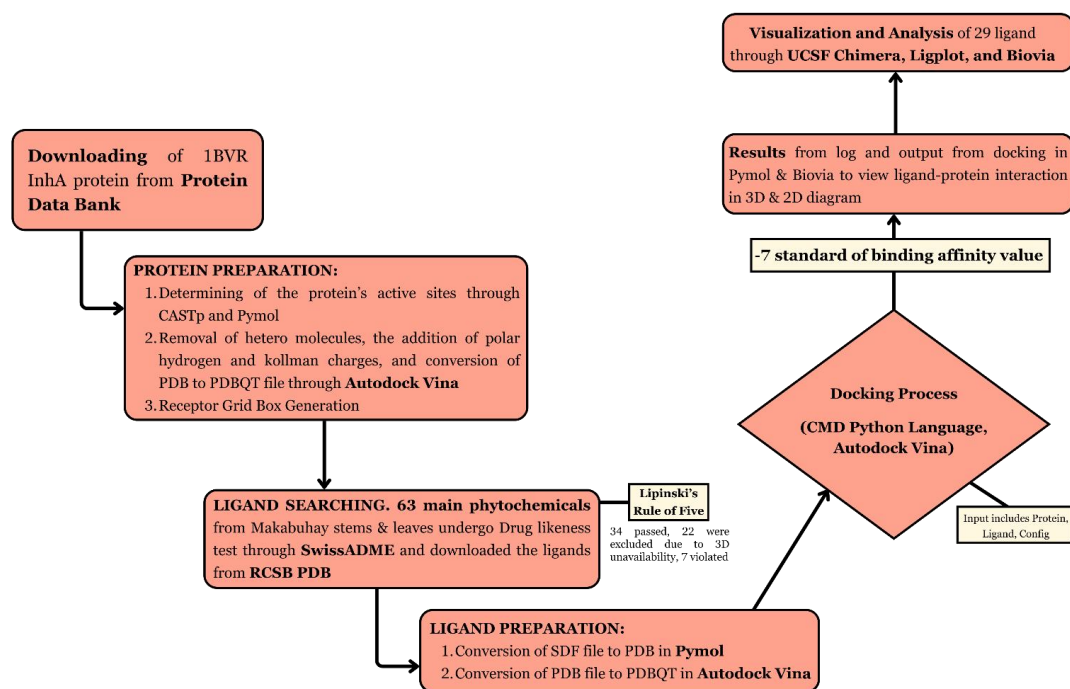
Methodological Framework

Fig 3. Methodological Framework of the study.

3. RESULTS AND DISCUSSIONS

This study aimed to determine and analyze the 63 primary phytochemical components obtained from *Tinospora crispa* (leaves and stem) targetting attachment active binding sites. 22 of the phytochemicals were not available which resulted in the reduction of the phytochemicals under consideration to 41. The 41 phytochemicals were subjected to SwissADME following the Lipinski rule, where the physicochemical properties of the phytochemical ligands were evaluated before the molecular docking procedure. Among the 41 phytochemicals, 34 were found to have passed Lipinski's rule of fifth.

Table 1: *Phytochemicals found in Makabuhay*

a	b	c	d	e	f
Apigenin	270.24	3	5	0.52	0
Diosmetin	300.26	3	6	0.22	0
Genkwanin	284.26	2	5	0.77	0
Luteolin 4'-methyl ether 7-glucoside	462.4	6	11	-1.89	2
Cycloeucalenol	426.7	1	1	6.92	1

Cycloeucalenone	424.7	0	1	6.82	1
Tinocrispol A	388.41	2	7	1.10	0
Borapetol A	376.40	2	7	1.04	0
Borapetol B	390.43	2	7	1.18	0
Borapetoside A	538.5	5	12	-1.12	2
Borapetoside B	552.6	5	12	-1.01	2
Borapetoside C	536.6	4	11	-0.25	2
Borapetoside E	536.6	4	11	-0.25	2
Borapetoside F	534.6	4	11	-0.33	2
Syringin	372.37	5	9	-1.59	0
Columbin	358.39	1	6	1.76	0
Magnoflorine	342.41	2	4	-1.71	0
N-Formylanonaine	293.32	0	3	2.95	0
Phytol	456.70	1	1	5.25	1
Ursolic acid	456.70	2	3	5.82	1
N-acetylanonaine	307.34	0	3	2.78	0
Lysicamine	291.30	0	4	1.54	0
Tyramine	137.18	2	2	1.21	0
Higenamine	204.26	4	4	1.60	0
N-cis-feruloyltyramine	313.35	3	4	1.89	0
N-trans-feruloyltyramine	313.35	3	4	1.89	0
Paprazine	283.32	3	3	2.22	0
N-trans-caffeoyltyramine	299.32	4	4	1.65	0
Columbamine	338.38	1	4	1.78	0
Palmatine	352.40	0	4	2.01	0
Jatrorrhizine	338.38	1	4	1.78	0
Berberine	336.36	0	4	2.19	0
Salsolinol	179.22	3	3	0.83	0

(−)-Litcubinine	314.36	3	5	-1.90	0
Secoisolariciresinol	362.42	4	6	1.56	0
Syringaresinol	344.32	2	7	1.56	0
Adenosine	267.24	4	7	-2.72	0
Uridine	244.20	4	6	-2.24	0
Adenine	135.13	2	3	-1.23	0
B-sitosterol	414.71	1	1	6.73	1
Stigmasterol	412.69	1	1	6.62	1
Naringenin	272.25	3	5	0.71	0
4,7-Dihydroxyc oumarin	178.14	2	4	0.45	0
Scopoletin	192.17	1	2	0.76	0
Scopolin	354.31	4	9	-1.23	0
Makisterone A	494.66	6	7	1.33	1
Vanillin	152.15	1	3	0.51	0
Borapetoside D	698.71	7	16	-2.41	3

***a** = Ligands; **b** = MolecularWeight (g/mol, **<500**); **c** = Number of Hydrogen bond donors (**<5**); **d** = Number of Hydrogen bond acceptors(**<1**)*

Notably, seven of the 41 phytochemicals that were assessed violated Lipinski's rule of Fifth, which resulted in the reduction of the phytochemicals under consideration to 34. The 34 phytochemicals were subsequently docked with the control variables on 1BVR (Inha). A total of 5 repetitions were executed to ensure both consistency and precision. Afterward, the docking procedure generated five unique outputs and their corresponding reports; the output with the lowest binding affinity value was recorded for each iteration

Scoring Functions

In our molecular docking analysis, we used a binding affinity threshold of -7 kcal/mol as the basis for identifying potential ligands with high binding affinity to the 1BVR protein. This threshold was chosen because the first-line drug for tuberculosis (TB) has a binding affinity of -6.4 kcal/mol. By setting a higher benchmark of -7 kcal/mol, we aimed to focus on phytochemicals with a greater potential for interaction, which could lead to stronger inhibitory effects on the protein's function.

PyMOL was employed to visualize and identify the positions of five successful docking attempts that occupied the binding pocket of the 1BVR protein. This visual analysis helped confirm the proximity and orientation of the ligands relative to the active binding site, ensuring that their predicted interactions were meaningful in the context of the protein's structural conformation.

The docking simulations generated 34 ligand complexes, each representing a unique conformation of the phytochemicals. By analyzing their binding poses and affinities, we were able to narrow down the initial pool to 33 phytochemicals that met or exceeded the -7 kcal/mol threshold. Each of these ligand conformations was integrated into PDB files for further evaluation, with an emphasis on how they occupied the protein's binding pocket.

Among these phytochemicals, the one with the most negative binding affinity score was N-acetylnornuciferine, demonstrating the highest potential for binding to 1BVR. This was followed by Lysicamine Cycloeucalenone, and N-acetylanonaine, which also exhibited strong binding affinities. These results suggest that these specific phytochemicals may have higher chances of interacting with 1BVR and potentially inhibiting its activity, making them promising candidates for further investigation in therapeutic applications related to the heme degradation pathway or even in designing novel drugs for TB or related conditions.

Table 2: 32 Phytochemicals with -7.0 and Lower Binding Affinity Values

a	b	c	d
N-acetylnornuciferine	101630664	-13.1	output 2
Apigenin	5280443	-8.2	output 7
Diosmetin	5281612	-8.2	output 3
Genkwanin	5281617	-9.4	output 6
Cycloeucalenol	101690	-9.4	output 1
Cycloeucalenone	21594790	-9.8	output 3
Tinocrispol A	101558920	-8.0	output 8
Borapetol A	21636047	-9.1	output 2
Borapetol B	273582832	-8.3	output 7
Syringin	5316860	-7.1	output 9
Columbin	442015	-9.3	output 4
Magnoflorine	73337	-9.3	output 9
N-formylanonaine	158516	-9.7	output 5
Lysicamine	122691	-9.9	output 1
N-acetylanonaine	6453733	-9.8	output 2
Higenamine	114840	-8.3	output 6
N-cis-feruloyltyramine	6440659	-8.0	output 8
N-trans-feruloyltyramine	5280537	-8.0	output 6
Paprazine	5372945	-7.8	output 10
N-trans-caffeoyltyramine	9994897	-8.2	output 2
Columbamine	72310	-7.8	output 6
Jatrorrhizine	72323	-8.6	output 7
Palmatine	19009	-7.7	output 8
Adenosine	60961	-7.0	output 8
Berberine	2353	-8.8	output 5
Salsolinol	91588	-7.7	output 2
(−)-Litcubinine	85190560	-8.6	output 1
Secoisolariciresinol	65373	-7.9	output 5
Syringaresinol	100067	-8.3	output 2
B-sitosterol	222284	-8.5	output 9
Stigmasterol	5280794	-9.5	output 2
Makisterone C	24984905	-9.5	output 6

a = phytochemical name; b = CID from PUBCHEM (<5); c = binding affinity values; d = output number

Protein and Ligand Interactions between interacting residues

The protein-ligand interactions between the phytochemicals and the active residues of the 1BVR protein revealed significant binding patterns, primarily driven by hydrogen bonds, hydrophobic interactions, and π-π stacking. Among the ligands, N-acetylnornuciferine exhibited the strongest binding

affinity, followed by N-acetylanonaine and Lysicamine, all of which surpassed the standardized threshold of -7 kcal/mol, indicating a higher likelihood of effective interaction. These ligands formed key interactions with residues like Serine, Valine, and Tyrosine, which are crucial for maintaining binding stability. Hydrophobic interactions with non-polar residues and hydrogen bonds with polar amino acids further stabilized these ligands within the binding pocket, enhancing their potential as inhibitors of 1BVR.

Given that the first-line drug for tuberculosis has a binding affinity of -6.4 kcal/mol, we used -7 kcal/mol as a baseline for identifying phytochemicals with superior binding potential. The visualization in PyMOL confirmed that five ligand conformations consistently occupied the binding pocket, supporting their interaction potential. These phytochemicals, particularly N-acetylnornuciferine, demonstrated binding affinities stronger than the reference drug, making them promising candidates for further study. The results highlight the importance of non-covalent interactions in ligand binding, positioning these compounds as potential leads for tuberculosis treatment, particularly by inhibiting the activity of 1BVR.

Table 2: 32 Phytochemicals with -7.0 and Lower Binding Affinity Values

a	b	c
N-acetylnornuciferine	*N/A*	*ALA154*
		THR162
		MET155
		ASN159
		PHE108
		PHE109
Apigenin	**GLY96(A)**	**PHE97**
	[3.06, 3.16, 2.86]	**PHE41**
	GLY14(A)	**ILE16**
	[3.33]	**ILE95**
	LEU63(A)	**ILE15**
	[3.16]	**GLY14**
Genkwanin	*GLY14*	**PHE97**
	[3.12]	*THR39*
	VAL65	*GLY40*
	[2.90]	*SER13*
		LEU63
		ASP64
		ILE122
		PHE41
		GLY96
Cycloeucalenol	*N/A*	*SER94*
		GLY14
		ILE16
		PHE41
		ILE95
		ASP64
		VAL65
		ILE122

		GLY96
		ILE21
Cycloeucalenone	*N/A*	*ILE21*
		SER20
		ILE122
		GLY14
		PHE41
		LEU63
		ILE95
		VAL65
		ILE16
		GLY96
		THR196
Tinocrispol A	*VAL65(A)*	*ASP64*
	[3.19]	*LEU63*
		PHE97
		ILE16
		ARG43
		PHE41
		GLY96
		ILE22
		ILE95
Borapetol A	*GLY96(A)*	*ILE95*
	[3.00]	*ILE16*
Borapetol B	*TYR158(A)*	*MET103*
	[2.86]	*PHE149*
	THR196	*MET199*
	[2.99]	*LYS165*
	SER19(A)	*MET147*
	[3.28]	*ILE95*
	ILE21(A)	*SER94*
	[2.82]	*GLY96*
		SER20
Syringin	*ILE21*	*MET199*
	[3.17]	*ILE194*
	SER94	*PHE149*
	[2.96, 3.04, 3.18]	*ALA191*
	LYS165	*GLY192*

	[3.30]	*TYR158*
	THR196	*PRO193*
	[2.96, 2.80]	*MET147*

Columbin	*THR196*	**GLY192**
	[3.14]	*MET147*
		LYS165
		PHEL149
		TYR158
		MET199
		PRO193
		ILE194
		ILE21
		ASP148
Magnoflorine	*THR196*	**ILE21**
	(3.12)	**GLY192**
		MET147
		PHE149
		LYS165
		ASP148
		TYR158
		MET199
		PRO193
		ILE194
N-formylanonaine	*N/A*	*VAL65*
		ASP64
		ILE122
		PHE41
		ILE16
		GLY40
		GLY14
		THR39
		SER13
		LEU63
		ILE95

Compound		Residues
Lysicamine	*N/A*	***ASP64***
		ILE122
		ILE16
		GLY14
		SER13
		THR39
		LEU63
		ILE95
		VAL65
		PHEL41
N-acetylanonaine	*GLY14*	***ILE22***
	[3.21]	***PHE41***
		ILE95
		LEU63
		VAL65
		SER13
		GLY40
		THR39
		ILE16
		PHE97
Higenamine	*THR39*	*GLY40*
	[3.07]	***ILE95***
	GLY14	***ILE122***
	[2.96]	***PHE41***
	LEU63	*ILE16*
	[2.89]	
N-cis-feruloyltyramine	***GLY14***	*LEU63*
	[3.04]	*PHE41*
	ILE15	*ILE95*

	[2.85]	*THR196*
	GLY96	*SER20*
	[3.04]	**ILE16**
	ILE21	**SER94**
	[2.91]	**GLY40**
		SER13
N-trans-feruloyltyramine	*VAL65*	*THR39*
	[2.97]	*GLY40*
	LEU63	**ILE95**
	[3.00]	*SER94*
		ILE21
		THR196
		GLY14
		ASP64
		PHE41
Paprazine	*LEU63*	**ASP64**
	[2.93]	**PHE41**
	VAL65	*SER94*
	[2.85]	*GLY14*
	ILE21	**SER20**
	[3.00]	**THR196**
		ILE16
		ILE122
N-trans-caffeoyltyramine	*LEU63*	**ILE122**
	[2.80]	*GLY14*
	VAL65	**SER20**
	[3.09]	**THR196**
	SER94	*ILE16*

	[2.83]	***ASP64***
	ALA22	***PHE41***
	[3.23]	
	ILE21	
	[3.22, 2.99]	
Columbamine	*ILE15*	***PHE97***
	[2.83]	*GLY96*
		ILE95
		THR39
		SER13
		LEU63
		GLY14
		PHE41
		GLY40
		ILE16
Jatrorrhizine	*VAL65*	***THR196***
	[2.89]	*GLY14*
	LEU63	***ILE95***
	[2.99]	*THR39*
		GLY40
		PHE41
		ASP64
Palmatine	**N/A**	ILE21
		MET103
		PRO156
		TYR158
		LEU218
		ALA157
		ILE215
		PHE149
		MET199
		GLY192
		ALA191
Adenosine	*GLY96*	***PHE97***
	[3.16, 2.86, 3.06]	*ILE16*
	LEU63	***PHE41***

		ILE15
	GLY14	GLY40
	[3.33]	**ILE95**
Berberine	GLY14	THR39
	[3.18]	**LEU63**
		ILE95
		ILE122
		GLY96
		PHE97
		ILE16
		SER13
		PHE41
		GLY40
Salsolinol	GLY14	SER13
	[3.01]	**THR39**
	LEU63	**ILE95**
	[2.91]	GLY40
		VAL65
		PHE41
		ILE122
(−)-Litcubinine	ILE15	**PHE97**
	[3.01, 308]	**GLY96**
	THR39	**PHE41**
	[3.09]	**LEU63**
		ILE95
		SER13
		GLY14
		GLY40
		ILE16
Secoisolariciresinol	ILE15	SER13
	[2.87]	GLY40
	THR39	**LEU63**
	[3.23]	**ILE95**
	GLY96	**ILE122**
	[3.04]	**PHE41**
		LYS118
		PHE97
		GLY14
		VAL65
Syringaresinol	**ALA198**	VAL65
	[3.22]	ASP64
	GLY14	PHE41
	[3.01]	ILE122

		ILE16
		THR196
		LEU197
		GLY96
		ILE95
		SER13
		THR39
		GLY40
		LEU63
B-sitosterol	*LEU63(A)*	*GLY14*
		GLY96
		PHE41
		MET98
		PRO99
		GLN100
		PHE97
		ILE95
		ILE16
Stigmasterol	*N/A*	*ILE21*
		GLY96
		SER94
		ILE95
		ILE122
		VAL65
		LEU63
		PHE41
		ILE16
		GLY14
		THR196

A	b	c
Makisterone C	*ASP148*	**ILE21**
	[3.23, 2.70]	**PHE149**
	ALA191	**MET147**
	[3.18]	*GLY96*
	GLY14	*ILE16*
	[2.70, 292]	*ILE15*
	SER94	**ILE95**
	[2.94]	**SER20**
		TYR158
		LYS165
		THR196
Syringaresinol	**ALA198**	*VAL65*
	[3.22]	*ASP64*
	GLY14	*PHE41*
	[3.01]	*ILE122*
		ILE16
		THR196
		LEU197
		GLY96
		ILE95
		SER13
		THR39
		GLY40
		LEU63

A = phytochemical name; b = residues; c = Hydrophobic residues; bold = binding sites of hydrogen bonds with interacting interactions with interacting ephrin B2/B3

Overview of Leading Ligands

N-acetylnornuciferine, N-acetylanonaine are the leading The ligands exhibited a diverse affinities, wherein N-highest value of -13.1 kcal/mol, 9.9 kcal/mol. The binding including Cycloeucalenone and underscore their potential as protein associated with

Lysicamine, Cycloeucalenone, and ligands according to this ranking. array of remarkable binding acetylnornuciferine exhibited the closely followed by Lysicamine at - affinities of the remaining ligands,

N-acetylanonaine at -9.8 kcal/mol, effective inhibitors of the 1BVR Mycobacterium tuberculosis.

The consistent outcomes from potency of these compounds' interactions with critical residues 1BVR protein. The insights value in advancing the possible antitubercular agents, comprehension of their assessment of each compound's evaluating their respective involvement of interactive bonds and hydrophobic

this docking analysis highlight the binding and their specific implicated in the inhibition of the provided by this data are of great investigation of these ligands as thereby enhancing our therapeutic capabilities. The inhibitory potential relied heavily on binding affinity levels and the residues, encompassing hydrogen interactions among the molecules.

Binding affinity within molecular the interaction occurring at a ligand and a receptor, foretelling association. Notably, the

docking denotes the robustness of specific binding site between a the probability and strength of their substantial contributions of

hydrogen bonds and hydrophobic interactions significantly impact the efficacy of the phytochemicals from Tinospora crispa in binding to the 1BVR protein. These interactions, which are essential for ligand-protein binding, often synergistically facilitate high binding affinity and specificity in targeting proteins.

N-acetylnornuciferine demonstrated interactions with several pivotal binding sites on the 1BVR protein, specifically engaging with residues such as Ser152 and Arg153. This compound established two strong hydrogen bonds—one with Gly14 at a distance of 3.21 Å and another with Asp64 at a distance of 2.89 Å. Additionally, the hydrophobic interactions with residues like Val65 and Ile95 enhanced its binding stability. Such characteristics position N-acetylnornuciferine as the most promising inhibitor of the 1BVR protein, supporting its role in antitubercular therapy.

Top Four Phytochemicals with the Most Interacting Residues

The top four phytochemicals identified in the study based on their binding interactions and affinities are N-acetylnornuciferine, Lysicamine, Cycloeucalenone, and N-acetylanonaine. N-acetylnornuciferine exhibited the strongest binding affinity of -13.1 kcal/mol, interacting with six key residues in the 1BVR protein, including Ser152 and

Arg153. This compound established two strong hydrogen bonds with Gly14 and Asp64, which contributed significantly to its stability. The robust hydrophobic interactions with non-polar residues, such as Val65 and Ile95, further enhanced its binding efficacy, positioning N-acetylnornuciferine as a promising candidate for inhibiting Mycobacterium tuberculosis.

Following closely behind, Lysicamine demonstrated a binding affinity of -9.9 kcal/mol and formed significant interactions with residues such as Asp64 and Gly14. The hydrogen bonds formed between Lysicamine and these residues contributed significantly to its stability, making it another viable candidate for further research. Cycloeucalenone ranked third, exhibiting a binding affinity of -9.8 kcal/mol with crucial interactions involving Ile21, Gly14, and Ser20. The compound's ability to form both hydrogen bonds and hydrophobic interactions allows it to maintain a stable binding profile, reinforcing its potential as an inhibitor. Lastly, N-acetylanonaine, also exhibiting a binding affinity of -9.8 kcal/mol, showed significant interactions with Gly14 and Phe41, forming stable hydrogen bonds and hydrophobic contacts that contribute to its effectiveness as an inhibitor.

Other Phytochemicals with Notable Interacting Residues

In addition to the top four ligands, several other phytochemicals demonstrated notable binding interactions with the 1BVR protein. Stigmasterol, for instance, showed a binding affinity of -9.5 kcal/mol and engaged with residues such as Ile21, Gly96, and Ser94. Although it did not form strong hydrogen bonds, the hydrophobic interactions with key residues helped ensure that Stigmasterol remained effectively bound to the protein, making it a compound worth further investigation.

Genkwanin, with a binding affinity of -9.4 kcal/mol, formed hydrogen bonds with Gly14 and Val65, providing moderate stability through interactions at distances of 3.12 Å and 2.90 Å. Hydrophobic interactions with residues such as Phe97, Ser13, and Leu63 further enhanced its binding stability. Although Genkwanin ranked lower than the top four ligands, its strong binding interactions suggest that it could serve as a potent inhibitor.

Borapetol B exhibited a binding affinity of -8.3 kcal/mol, interacting with several key residues, including Gly14 and Ser94. The formation of a

hydrogen bond with Ser94 at a distance of 3.08 Å was significant for maintaining stability. Additionally, its hydrophobic interactions with residues such as Ile21 and Phe149 suggest that Borapetol B could still serve as a viable inhibitor, especially when used in combination with other compounds.

Lastly, Makisterone C was another phytochemical that exhibited notable binding potential, with a binding affinity of -9.5 kcal/mol. It formed several hydrophobic interactions with residues such as Ile21 and Gly96, which provided significant stability to the ligand-protein complex. In addition to its hydrophobic interactions, Makisterone C established a hydrogen bond with Asp148 at a distance of 3.23 Å, contributing to its overall binding strength. While it did not rank among the top four compounds, its balanced interaction profile suggests that Makisterone C could still be an effective inhibitor, particularly when used in a multi-target approach.

Across all the top-performing phytochemicals, hydrophobic interactions played a critical role in stabilizing the ligands. N-acetylnornuciferine, Lysicamine, Cycloeucalenone, and N-acetylanonaine each formed extensive hydrophobic contacts with non-polar residues such as Val65, Ile95, and Leu63. These interactions are crucial for stabilizing the ligands within the protein's hydrophobic binding pocket, preventing water molecules from disrupting the binding. The strength of these hydrophobic interactions across the top-performing ligands underscores their importance in maintaining stable ligand-protein complexes.

While hydrogen bonding was less frequent than hydrophobic interactions, it played a crucial role in enhancing specificity and stabilizing the ligand-protein complexes. N-acetylnornuciferine and Lysicamine formed hydrogen bonds with key residues such as Gly14 and Asp64, providing the specificity necessary for stable binding within the 1BVR protein. The lengths of these bonds, ranging from 2.70 Å to 3.12 Å, were optimal for maintaining robust interactions without compromising flexibility.

The docking results indicate that the top-performing phytochemicals from Tinospora crispa possess strong binding affinities and robust interaction profiles, combining hydrogen bonds and hydrophobic contacts to form stable ligand-protein complexes. The ability of these ligands to engage multiple residues, both polar and non-polar, suggests that they have high potential as inhibitors of Mycobacterium tuberculosis. This analysis provides a foundation for further exploration of these compounds as promising candidates for tuberculosis therapy.

Visualization of the top four Phytochemicals with the most interacting residues
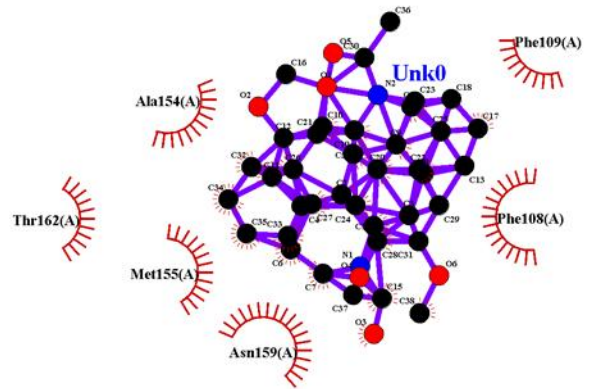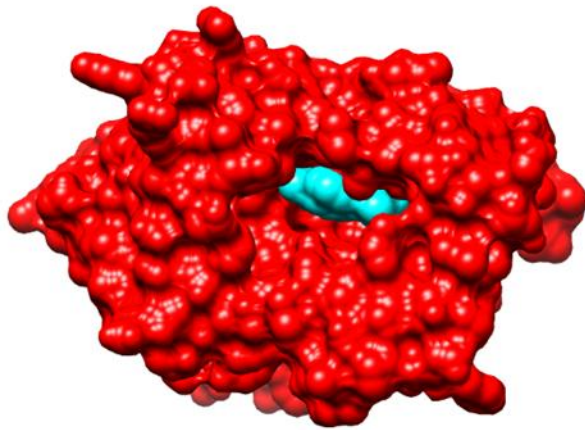
Figure 4. N-acetylnornuciferine-1BVR complex. Chimera 3D visualization (left); Ligplot+ hydrogen bonds and hydrophobic interactions 2D visualization (right).
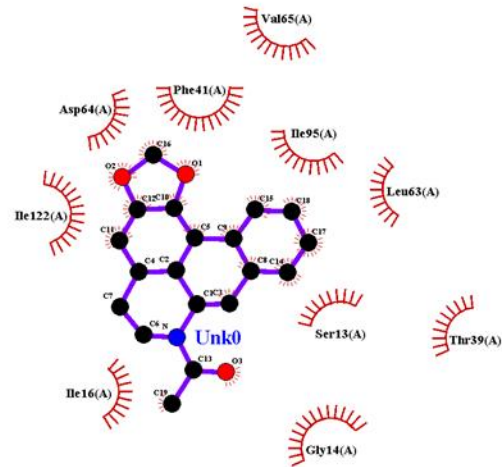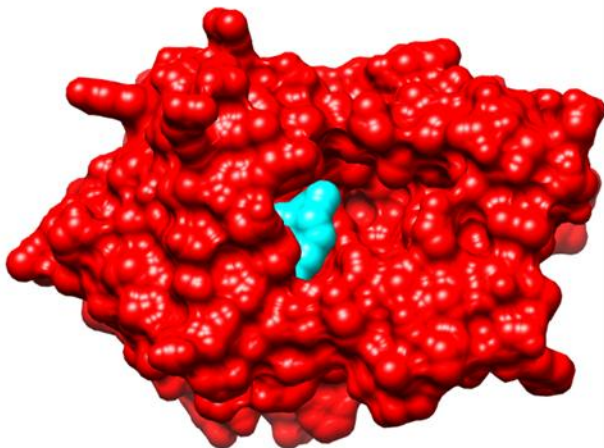
Figure 5. Lysicamine-1BVR complex. Chimera 3D visualization (left); Ligplot+ hydrogen bonds and hydrophobic interactions 2D visualization (right).
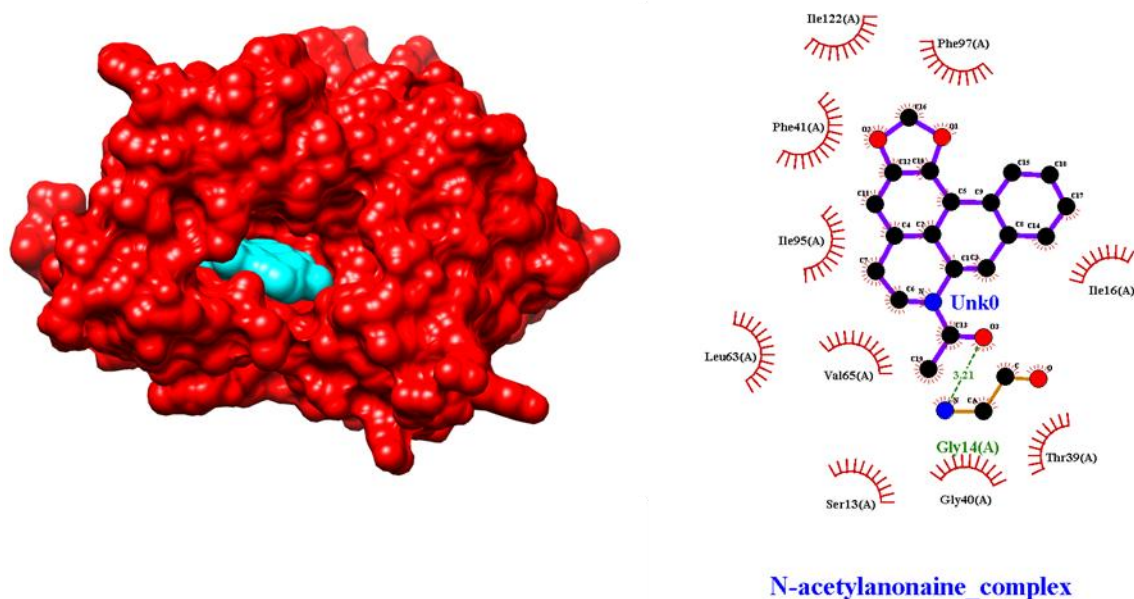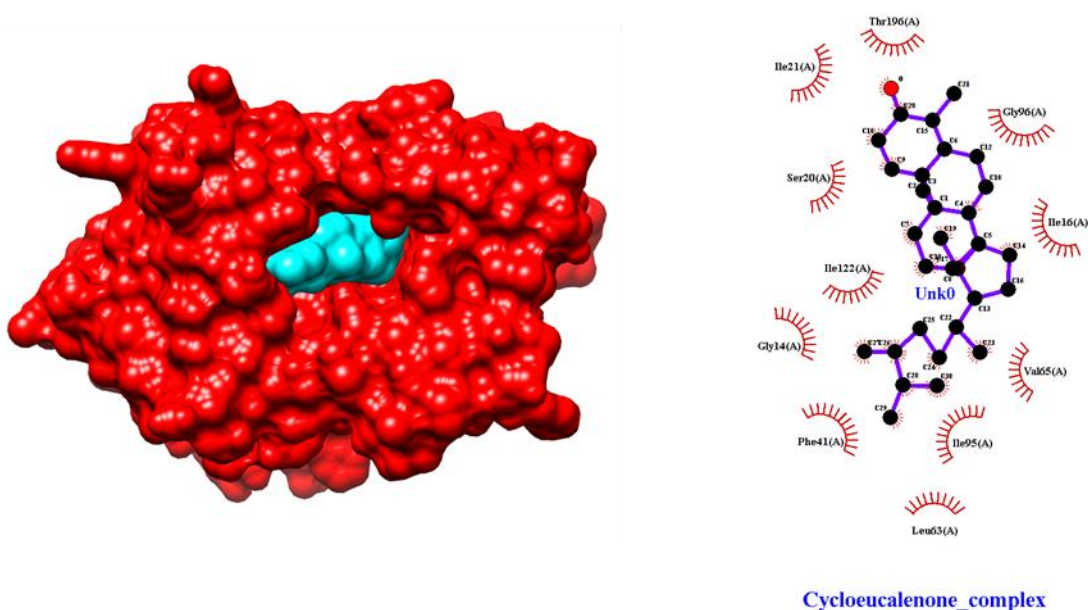
Figure 6. N-acetylanonaine-1BVR complex. Chimera 3D visualization (left); Ligplot+ hydrogen bonds and hydrophobic interactions 2D visualization (right).

Figure 7. Cycloeucalenone-1BVR complex. Chimera 3D visualization (left); Ligplot+ hydrogen bonds and hydrophobic interactions 2D visualization (right).

Conclusions and Recommendations

In conclusion, the molecular docking study of phytochemicals derived from Tinospora crispa revealed several promising candidates for inhibiting the 1BVR protein associated with Mycobacterium tuberculosis. Among the compounds evaluated, N-acetylnornuciferine exhibited the strongest binding affinity, indicating its significant potential as a lead compound for further development as an antitubercular agent. The binding interactions of this ligand with critical residues in the protein highlight its capability to effectively interfere with the function of Mycobacterium tuberculosis, making it a target for subsequent in vitro and in vivo studies.

The study identified Lysicamine, Cycloeucalenone, and N-acetylanonaine as other top contenders with strong binding affinities. Their interactions with the 1BVR protein and the presence of significant hydrogen bonds and hydrophobic contacts suggest that they may also serve as effective inhibitors.

Further exploration of these compounds could lead to the identification of new therapeutic options for treating tuberculosis, especially considering the rising rates of drug-resistant strains.

While this study provided valuable insights into the binding affinities and interactions of various phytochemicals, it is essential to validate these findings through experimental methods. Future research should focus on conducting in vitro assays using relevant Mycobacterium tuberculosis strains to assess the actual inhibitory effects of these compounds on bacterial growth and survival. Such studies will provide a clearer understanding of the pharmacological potential of these phytochemicals and their mechanisms of action.

Additionally, it would be beneficial to perform molecular dynamics simulations to investigate the stability and behavior of the ligand-protein complexes over time. This will help to elucidate the dynamic nature of the interactions and provide insights into the long-term efficacy of these compounds as therapeutic agents. Moreover, studying the pharmacokinetics and bioavailability of these ligands will be crucial for evaluating their potential as drug candidates.

To facilitate the transition from in silico studies to clinical applications, collaboration with experts in pharmacology and medicinal chemistry is recommended. This interdisciplinary approach can aid in the optimization of the identified compounds, leading to the development of derivatives with enhanced efficacy and safety profiles.

In summary, the promising results from this molecular docking study pave the way for further research into the antitubercular potential of Tinospora crispa phytochemicals. By advancing our understanding of these compounds through experimental validation and interdisciplinary collaboration, we can contribute to the development of novel therapeutic strategies against tuberculosis, addressing the urgent need for effective treatments in the face of rising drug resistance.

References:

Abdelaziz, O. A., Othman, D. I., Abdel-Aziz,M. M., Badr, S. M., & Eisa, H. M. (2022). Novel diaryl ether derivatives as InhA inhibitors: Design, synthesis and antimycobacterial activity. Bioorganic Chemistry, 129, 106125. https://doi.org/10.1016/j.bioorg.2022.106125

Abood, W. N., Fahmi, I., Abdulla, M. A., & Ismail, S. (2014). Immunomodulatory effect of an isolated fraction from Tinospora crispa on intracellular expression of INF-γ, IL-6 and IL-8. BMC Complementary and Alternative Medicine, 14(1). https://doi.org/10.1186/1472-6882-14-205

Alcaraz, M., Roquet-Banères, F., Leon-Icaza, S. A., Abendroth, J., Boudehen, Y., Cougoule, C., Edwards, T. E., & Kremer, L. (2022). Efficacy and Mode of Action of a Direct Inhibitor of Mycobacterium abscessus InhA. ACS Infectious Diseases, 8(10), 2171–2186. https://doi.org/10.1021/acsinfecdis.2c00314

Armstrong, T., Lamont, M., Lanne, A., Alderwick, L. J., & Thomas, N. R. (2020). Inhibition of Mycobacterium tuberculosis InhA: Design, synthesis and evaluation of new di-triclosan derivatives. Bioorganic & Medicinal Chemistry, 28(22), 115744. https://doi.org/10.1016/j.bmc.2020.115744

Bagcchi, S. (2022). WHO's Global Tuberculosis Report 2022. *The Lancet Microbe*, *4*(1), e20. https://doi.org/10.1016/s2666-5247(22)00359-7

Beltran, M. a. G., Robertson, A., & Martin, R. J. (2019). The Effects of Plant Leaves Variants from The Philippines on Infective Oesophagustonum dentatum Larvae. Veterinary Biomedical and Clinical Journal, 1(1), 9–18. https://doi.org/10.21776/ub.vetbioclinj.2019.001.01.2

Caraux-Paz, P., Diamantis, S., De Wazières, B., & Gallien, S. (2021). Tuberculosis in the elderly. Journal of Clinical Medicine, 10(24), 5888. https://doi.org/10.3390/jcm10245888

Chakaya, J., Khan, M., Ntoumi, F., Aklillu, E., Fatima, R., Mwaba, P., Kapata, N., Mfinanga, S., Hasnain, S. E., Katoto, P. D., Bulabula, A. N., Sam-Agudu, N. A., Nachega, J. B., Tiberi, S., McHugh, T. D., Abubakar, I., & Zumla, A. (2021). Global Tuberculosis Report 2020 – Reflections on the

Global TB burden, treatment and prevention efforts. International Journal of Infectious Diseases, 113, S7–S12. https://doi.org/10.1016/j.ijid.2021.02.107

Chebaiki, M., Delfourne, E., Tamhaev, R., Danoun, S., Rodriguez, F., Hoffmann, P., Grosjean, E., Goncalves, F., Azéma-Despeyroux, J., Pál, A., Korduláková, J., Preuilh, N., Britton, S., Constant, P., Marrakchi, H., Maveyraud, L., Mourey, L., & Lherbet, C. (2023). Discovery of new diaryl ether inhibitors against Mycobacterium tuberculosis targeting the minor portal of InhA. European Journal of Medicinal Chemistry, 259, 115646. https://doi.org/10.1016/j.ejmech.2023.115646

Chetty, S., Armstrong, T., Kharkwal, S. S., Drewe, W. C., De Matteis, C. I., Evangelopoulos, D., Bhakta, S., & Thomas, N. R. (2021). New INHA inhibitors based on expanded triclosan and Di-Triclosan analogues to develop a new treatment for tuberculosis. Pharmaceuticals, 14(4), 361. https://doi.org/10.3390/ph14040361

Conradie, F., Diacon, A. H., Ngubane, N., Howell, P., Everitt, D., Crook, A. M., Mendel, C. M., Egizi, E., Moreira, J., Timm, J., McHugh, T. D., Wills, G. H., Bateson, A., Hunt, R., Van Niekerk, C., Li, M., Olugbosi, M., & Spigelman, M. (2020). Treatment of Highly Drug-Resistant Pulmonary Tuberculosis. New England Journal of Medicine, 382(10), 893–902. https://doi.org/10.1056/nejmoa1901814

Deutsch-Feldman, M., Pratt, R. H., Price, S. F., Tsang, C. A., & Self, J. L. (2021). Tuberculosis — United States, 2020. MMWR Morbidity and Mortality Weekly Report, 70(12), 409–414. https://doi.org/10.15585/mmwr.mm7012a1

Doğan, Ş. D., Gündüz, M. G., Doğan, H., Krishna, V. S., Lherbet, C., & Sriram, D. (2020). Design and synthesis of thiourea-based derivatives as Mycobacterium tuberculosis growth and enoyl acyl carrier protein reductase (InhA) inhibitors. European Journal of Medicinal Chemistry, 199, 112402. https://doi.org/10.1016/j.ejmech.2020.112402

Espinosa-Pereiro, J., Sánchez-Montalvá, A., Aznar, M. L., & Espiau, M. (2022). MDR tuberculosis Treatment. Medicina, 58(2), 188. https://doi.org/10.3390/medicina58020188

Esquilla, M. G., Sanchez, C. B., & Tenorio, J. C. B. (2021). Molluscicidal activity of Makabuhay (Tinospora rumphii Boerl) stem ethanolic extract against Radix (Lymnaea) spp. snails. Journal on New Biological Reports, 10(2), 64-71.

Flint, L., Korkegian, A., & Parish, T. (2020). InhA inhibitors have activity against non-replicating Mycobacterium tuberculosis. PLoS ONE, 15(11), e0239354. https://doi.org/10.1371/journal.pone.0239354

Gatmaitan, J. G., Gatmaitan-Dumlao, J. K. G., Dayrit, J., & Gabriel, M. T. (2023). Efficacy and Safety of Makabuhay (Tinospora rumphii) 25% Cream Versus Hydrocortisone 1% Cream in the Management of Mosquito Bite Reactions: Randomized Double-Blind Controlled Trial. JMIR Dermatology, 6, e50380. https://doi.org/10.2196/50380

Gill, C. M., Dolan, L., Piggott, L. M., & McLaughlin, A. M. (2022). New developments in tuberculosis diagnosis and treatment. *Breathe*, *18*(1), 210149. https://doi.org/10.1183/20734735.0149-2021

Gong, W., & Wu, X. (2021). Differential diagnosis of latent tuberculosis infection and active tuberculosis: A key to a successful tuberculosis control Strategy. Frontiers in Microbiology, 12. https://doi.org/10.3389/fmicb.2021.745592

Haque, E., Bari, M. S., Khandokar, L., Anjum, J., Jantan, I., Seidel, V., & Haque, M. A. (2022). An updated and comprehensive review on the ethnomedicinal uses, phytochemistry, pharmacological activity and toxicological profile of Tinospora crispa (L.) Hook. f. & Thomson. Phytochemistry Reviews, 22(1), 211–273. https://doi.org/10.1007/s11101-022-09843-y

Harding, E. (2019). WHO global progress report on tuberculosis elimination. The Lancet Respiratory Medicine, 8(1), 19. https://doi.org/10.1016/s2213-2600(19)30418-7

Jain, V. K., Iyengar, K. P., Samy, D. A., & Vaishya, R. (2020). Tuberculosis in the era of COVID-19 in India. Diabetes & Metabolic Syndrome Clinical Research & Reviews, 14(5), 1439–1443. https://doi.org/10.1016/j.dsx.2020.07.034

Jayaraman, M., Loganathan, L., Muthusamy, K., & Ramadas, K. (2021). Virtual screening assisted discovery of novel natural products to inhibit the catalytic mechanism of Mycobacterium tuberculosis InhA. Journal of Molecular Liquids, 335, 116204. https://doi.org/10.1016/j.molliq.2021.116204

Kamsri, P., Hanwarinroj, C., Phusi, N., Pornprom, T., Chayajarus, K., Punkvang, A., Suttipanta, N., Srimanote, P., Suttisintong, K., Songsiriritthigul, C., Saparpakorn, P., Hannongbua, S., Rattanabunyong, S., Seetaha, S., Choowongkomon, K., Sureram, S., Kittakoop, P., Hongmanee, P., Santanirand, P., . . . Pungpo, P. (2019). Discovery of new and potent INHA inhibitors as antituberculosis agents: Structure-Based virtual screening validated by biological assays and x-ray crystallography. Journal of Chemical Information and Modeling, 60(1), 226–234. https://doi.org/10.1021/acs.jcim.9b00918

Khan, M., Khan, S., Alshammary, F. L., Zaidi, S., Singh, V., Ahmad, I., Patel, H., Gupta, V. K., & Haque, S. (2023). In silico analysis to identify potential antitubercular molecules in Morus alba through virtual screening and molecular dynamics simulations. Journal of Biomolecular Structure and Dynamics, 1–8. https://doi.org/10.1080/07391102.2023.2209648

Lange, C., Dheda, K., Chesov, D., Mandalakas, A. M., Udwadia, Z., & Horsburgh, C. R. (2019). Management of drug-resistant tuberculosis. The Lancet, 394(10202), 953–966. https://doi.org/10.1016/s0140-6736(19)31882-3

Lee, A., Xie, Y. L., Barry, C. E., & Chen, R. Y. (2020). Current and future treatments for tuberculosis. BMJ, m216. https://doi.org/10.1136/bmj.m216

MacLean, E., Kohli, M., Weber, S. F., Suresh, A., Schumacher, S. G., Denkinger, C. M., & Pai, M. (2020). Advances in Molecular diagnosis of tuberculosis. Journal of Clinical Microbiology, 58(10). https://doi.org/10.1128/jcm.01582-19

Migliori, G. B., Ong, C. W., Petrone, L., D'Ambrosio, L., Centis, R., & Goletti, D. (2021). The definition of tuberculosis infection based on the spectrum of tuberculosis disease. Breathe, 17(3), 210079. https://doi.org/10.1183/20734735.0079-2021

Mk, K., Mn, I., J, F., & Mm, A. (2019, January 1). An overview on epidemiology of tuberculosis. Abstract - Europe PMC. https://europepmc.org/article/med/30755580

Motta, I., Boeree, M., Chesov, D., Dheda, K., Günther, G., Horsburgh, C. R., Kherabi, Y., Lange, C., Lienhardt, C., McIlleron, H. M., Paton, N. I., Stagg, H. R., Thwaites, G., Udwadia, Z., Van Crevel, R., Velásquez, G. E., Wilkinson, R. J., Guglielmetti, L., Motta, I., . . . Guglielmetti, L. (2023). Recent advances in the treatment of tuberculosis. Clinical Microbiology and Infection. https://doi.org/10.1016/j.cmi.2023.07.013

Natarajan, A., Beena, P., Devnikar, A. V., & Mali, S. (2020). A systemic review on tuberculosis. *Indian Journal of Tuberculosis*, *67*(3), 295–311. https://doi.org/10.1016/j.ijtb.2020.02.005

Pascual, J. L., Reyes, C., Aliazas, J. V., & Panoy, J. F. D. (2024, June 27). Bioactive Components of Allium sativum (L.) and Tinospora crispa (L.) as Organic Molluscicidal Agents. TWIST Journal. https://twistjournal.net/twist/article/view/315

Paton, N. I., Cousins, C., Suresh, C., Burhan, E., Chew, K. L., Dalay, V. B., Lu, Q., Kusmiati, T., Balanag, V. M., Lee, S. L., Ruslami, R., Pokharkar, Y., Djaharuddin, I., Sugiri, J. J., Veto, R. S., Sekaggya-Wiltshire, C., Avihingsanon, A., Sarin, R., Papineni, P., . . . Crook, A. M. (2023). Treatment strategy for Rifampin-Susceptible tuberculosis. New England Journal of Medicine, 388(10), 873–887. https://doi.org/10.1056/nejmoa2212537

Peloquin, C. A., & Davies, G. R. (2021). The treatment of tuberculosis. Clinical Pharmacology & Therapeutics, 110(6), 1455–1466. https://doi.org/10.1002/cpt.2261

Phusi, N., Hashimoto, Y., Otsubo, N., Imai, K., Thongdee, P., Sukchit, D., Kamsri, P., Punkvang, A., Suttisintong, K., Pungpo, P., & Kurita, N. (2022). Structure-based drug design of novel M. tuberculosis InhA inhibitors based on fragment molecular orbital calculations. Computers in Biology and Medicine, 152, 106434. https://doi.org/10.1016/j.compbiomed.2022.106434

Pitaloka, D. a. E., Ramadhan, D. S. F., Arfan, N., Chaidir, L., & Fakih, T. M. (2021). Docking-Based Virtual Screening and Molecular Dynamics Simulations of Quercetin Analogs as Enoyl-Acyl Carrier Protein Reductase (InhA) Inhibitors of Mycobacterium tuberculosis. Scientia Pharmaceutica, 89(2), 20. https://doi.org/10.3390/scipharm89020020

Pitaloka, D. a. E., Arfan, A., Alfarafisa, N. M., Chaidir, L., & Supratman, U. (2023). Discovery of potent triterpenoid and limonoid compounds targeting Mycobacterium tuberculosis enoyl acyl carrier protein reductase (InhA): An in silico investigation. Informatics in Medicine Unlocked, 40, 101299. https://doi.org/10.1016/j.imu.2023.101299

Prasad, M. S., Bhole, R. P., Khedekar, P. B., & Chikhale, R. V. (2021). Mycobacterium enoyl acyl carrier protein reductase (InhA): A key target for antitubercular drug discovery. Bioorganic Chemistry, 115, 105242. https://doi.org/10.1016/j.bioorg.2021.105242

Raghu, Kumar, C. P., Kumar, K. Y., Prashanth, M., Alshahrani, M. Y., Ahmad, I., & Jain, R. (2022). Design, synthesis and molecular docking studies of imidazole and benzimidazole linked ethionamide derivatives as inhibitors of InhA and antituberculosis agents. Bioorganic & Medicinal Chemistry Letters, 60, 128604. https://doi.org/10.1016/j.bmcl.2022.128604

Rasheed, A. (2021). A review on the role of InhA inhibitors in Tuberculosis (TB). *J Med. Med. Sci Res*, *1*(1). Halder, S. K., & Elma, F. (2021). In silico identification of novel chemical compounds with antituberculosis activity for the inhibition of InhA and EthR proteins from Mycobacterium tuberculosis. Journal of Clinical Tuberculosis and Other Mycobacterial Diseases, 24, 100246. https://doi.org/10.1016/j.jctube.2021.100246

Reid, M. J. A., Arinaminpathy, N., Bloom, A., Bloom, B. R., Boehme, C., Chaisson, R., Chin, D. P., Churchyard, G., Cox, H., Ditiu, L., Dybul, M., Farrar, J., Fauci, A. S., Fekadu, E., Fujiwara, P. I., Hallett, T. B., Hanson, C. L., Harrington, M., Herbert, N., . . . Goosby, E. P. (2019). Building a tuberculosis-free world: The Lancet Commission on tuberculosis. The Lancet, 393(10178), 1331–1384. https://doi.org/10.1016/s0140-6736(19)30024-8

Rodriguez, F., Saffon, N., Sammartino, J. C., Degiacomi, G., Pasca, M. R., & Lherbet, C. (2019). First triclosan-based macrocyclic inhibitors of InhA enzyme. Bioorganic Chemistry, 95, 103498. https://doi.org/10.1016/j.bioorg.2019.103498

Roy, R. B., Whittaker, E., Seddon, J. A., & Kampmann, B. (2018). Tuberculosis susceptibility and protection in children. The Lancet Infectious Diseases, 19(3), e96–e108. https://doi.org/10.1016/s1473-3099(18)30157-9

Sabbah, M., Mendes, V., Vistal, R. G., Dias, D. M. G., Záhorszká, M., Mikušová, K., Korduláková, J., Coyne, A. G., Blundell, T. L., & Abell, C. (2020). Fragment-Based Design of Mycobacterium tuberculosis InhA Inhibitors. Journal of Medicinal Chemistry, 63(9), 4749–4761. https://doi.org/10.1021/acs.jmedchem.0c00007

Sawy, M. a. E., Elshatanofy, M. M., Kilany, Y. E., Kandeel, K., Elwakil, B. H., Hagar, M., Aouad, M. R., Albelwi, F. F., Rezki, N., Jaremko, M., & Ashry, E. S. H. E. (2022). Novel Hybrid 1,2,4- and 1,2,3-Triazoles targeting Mycobacterium tuberculosis enoyl acyl carrier protein reductase (INHA): design, synthesis, and molecular docking. International Journal of Molecular Sciences, 23(9), 4706. https://doi.org/10.3390/ijms23094706

Schrager, L. K., Vekemens, J., Drager, N., Lewinsohn, D. M., & Olesen, O. F. (2020). The status of tuberculosis vaccine development. The Lancet Infectious Diseases, 20(3), e28–e37. https://doi.org/10.1016/s1473-3099(19)30625-5

Schwartz, N. G., Price, S. F., Pratt, R. H., & Langer, A. J. (2020). Tuberculosis — United States, 2019. MMWR Morbidity and Mortality Weekly Report, 69(11), 286–289. https://doi.org/10.15585/mmwr.mm6911a3

Singh, K., Pandey, N., Ahmad, F., Upadhyay, T. K., Islam, M. H., Alshammari, N., Saeed, M., Al-Keridis, L. A., & Sharma, R. (2022). Identification of Novel Inhibitor of Enoyl-Acyl Carrier Protein Reductase (InhA) Enzyme in Mycobacterium tuberculosis from Plant-Derived Metabolites: An In Silico Study. Antibiotics, 11(8), 1038. https://doi.org/10.3390/antibiotics11081038

Stadler, J. a. M., Maartens, G., Meintjes, G., & Wasserman, S. (2023). Clofazimine for the treatment of tuberculosis. Frontiers in Pharmacology, 14. https://doi.org/10.3389/fphar.2023.1100488

Suárez, I., Fünger, S. M., Kröger, S., Rademacher, J., Fätkenheuer, G., & Rybniker, J. (2019). The diagnosis and treatment of tuberculosis. Deutsches Aerzteblatt International, 116(43).

Taylor & Francis. (n.d.). Facing Antitubercular Resistance: Identification of Potential Direct Inhibitors Targeting InhA Enzyme and Generation of 3D-pharmacophore Model by in silico Approach. https://www.tandfonline.com/doi/full/10.2147/AABC.S394535

Teneva, Y., Simeonova, R., Valcheva, V., & Angelova, V. T. (2023). Recent advances in Anti-Tuberculosis drug discovery based on Hydrazide–Hydrazone and thiadiazole derivatives targeting INHA. Pharmaceuticals, 16(4), 484. https://doi.org/10.3390/ph1604048

Turkova, A., Wills, G. H., Wobudeya, E., Chabala, C., Palmer, M., Kinikar, A., Hissar, S., Choo, L., Musoke, P., Mulenga, V., Mave, V., Joseph, B., LeBeau, K., Thomason, M. J., Mboizi, R. B., Kapasa, M., Van Der Zalm, M. M., Raichur, P., Bhavani, P. K., . . . Crook, A. M. (2022). Shorter treatment for nonsevere tuberculosis in African and Indian children. New England Journal of Medicine, 386(10), 911–922. https://doi.org/10.1056/nejmoa2104535

Venugopala, K. N., Chandrashekharappa, S., Deb, P. K., Tratrat, C., Pillay, M., Chopra, D., Al-Shar'i, N. A., Hourani, W., Dahabiyeh, L. A., Borah, P., Nagdeve, R. D., Nayak, S. K., Padmashali, B., Morsy, M. A., Aldhubiab, B. E., Attimarad, M., Nair, A. B., Sreeharsha, N., Haroun, M., . . . Mailavaram, R. (2021). Anti-tubercular activity and molecular docking studies of indolizine derivatives targeting mycobacterial InhA enzyme. Journal of Enzyme Inhibition and Medicinal Chemistry, 36(1), 1471–1486. https://doi.org/10.1080/14756366.2021.1919889

Vora, D., Upadhyay, N., Tilekar, K., Jain, V., & Ramaa, C. S. (2019). Development of 1,2,4-Triazole-5-Thione derivatives as potential inhibitors of enoyl acyl carrier protein reductase (INHA) in tuberculosis. PubMed, 18(4), 1742–1758. https://doi.org/10.22037/ijpr.2019.112039.13495

Wang, X., Perryman, A. L., Li, S., Paget, S. D., Stratton, T. P., Lemenze, A., Olson, A. J., Ekins, S., Kumar, P., & Freundlich, J. S. (2019). Intrabacterial Metabolism Obscures the Successful Prediction of an InhA Inhibitor of Mycobacterium tuberculosis. ACS Infectious Diseases, 5(12), 2148–2163. https://doi.org/10.1021/acsinfecdis.9b00295

World Health Organization. (2021). WHO consolidated guidelines on tuberculosis. Module 2: screening-systematic screening for tuberculosis disease. World Health Organization.Zimmer, A. J., Klinton, J. S., Oga-Omenka, C.,

Heitkamp, P., Nyirenda, C. N., Furin, J., & Pai, M. (2021). Tuberculosis in times of COVID-19. Journal of Epidemiology & Community Health, 76(3), 310–316. https://doi.org/10.1136/jech-2021-217529